A numerical and experimental study of the artificial freezing of sand

GIANCARLO GIODA
Department of Structural Engineering, Politecnico di Milano, Piazza L. da Vinci 32, 20133 Milano, Italy.
LIVIO LOCATELLI
Geocad s.r.l., Milano, Italy
AND
FRANCESCO GALLAVRESI
Rodio S.p.A., Casalmaiocco, Milano, Italy

Received October 22, 1992
Accepted September 13, 1993

A study is presented of the transfer of heat within a saturated sand with reference to the analysis of artificial freezing of the ground. First, the main characteristics of the adopted finite element approach and of the technique that introduces the latent-heat effects during the water–ice phase transition are illustrated. Subsequently, the results of some laboratory freezing tests are presented on the basis of which the computer program and the procedure for working out the thermal constants of the soil were calibrated. Finally, a parametric study is discussed that concerns the effects of pipe diameter, distance between pipes, and coolant temperature on the progress of the 0°C isotherm.

Key words: artificial freezing, finite elements, heat transfer, laboratory test, Stefan problem.

Une étude du transfert de chaleur dans un sable saturé en vue de l'analyse du gel artificiel du sol est présentée. En premier lieu les principales caractéristiques de l'approche d'éléments finis adoptée et de la technique qui introduit les effets de la chaleur latente durant la phase de transition eau–glace sont illustrées. Subséquemment, l'on présente les résultats d'essais de gel en laboratoire qui sont à la base de la calibration du programme d'ordinateur et de la procédure pour établir les constantes thermiques du sol. Finalement, l'on discute une étude paramétrique qui porte sur les effets du diamètre des tuyaux, de la distance entre eux, et de la température du réfrigérant sur le progrès de l'isotherme 0°C.

Mots clés : gel artificiel, éléments finis, transfert de chaleur, essai en laboratoire, problème de Stefan.
[Traduit par la rédaction]

Can. Geotech. J. 31, 1–11 (1994)

1. Introduction

Artificial freezing of the ground has been used for decades to improve the mechanical characteristics of soils for execution of large underground works in difficult geotechnical conditions (Sanger 1968; Andersland et al. 1989). In particular, ground freezing has been adopted in geotechnical, transportation, and mining engineering to assist in the construction of tunnels and shafts below the water table and for shallow excavations associated with large buildings.

This technique is based on the circulation of low-temperature fluids through pipes inserted in the ground and sometimes represents the only economical solution, compared to other methods, able to satisfy the geotechnical design requirements.

The development of artificial ground freezing has been largely influenced by advances in both research and technology. In fact, the theoretical and experimental research carried out in this field led to a deeper knowledge of the mechanical properties of frozen soil and of important effects induced by freezing (e.g., the volumetric deformation of soil), thus allowing development of practical procedures for design and control of the freezing systems (Frivik and Thorbergsen 1980). The technological advances were related to improved drilling techniques, monitoring systems, and cryogenic techniques and to the experience gained in successful completion of numerous projects.

It can be observed, however, that the "optimization" of some important parameters, such as the diameter of the freezing pipes, distance between the pipes, and the temperature of the coolant, has not been studied extensively despite their influence on the time and costs of the treatment and, hence, on the overall design of a ground-freezing system.

In this paper the results of a numerical and experimental study are presented with the objective of developing a numerical procedure for the analysis of freezing of saturated sands which could be adopted to optimize the freezing system through suitable parametric investigations.

The numerical analysis of the artificial freezing of saturated soils represents a nontrivial problem because of the complex mechanical and thermal phenomena involved, including the nonlinear conductive transfer of heat within the soil; the water–ice phase transition and the associated release of latent heat; the influence of water seepage on heat transfer; the volume increase of the frozen soil and the possible migration of water toward the freezing front; and the change of mechanical characteristics, in particular the shear strength and time-dependent frozen soil properties.

To reduce the complexity of the solution algorithm, the problem has been limited by considering only the thermal aspects and by introducing some simplifying assumptions. This reduces the analysis of freezing of saturated sands to the solution of the so-called Stefan problem, i.e., the transfer of heat by conduction while accounting for phase changes.

In choosing the technique for numerical solution both finite element and boundary integral equation methods were considered (Zabaras and Ruan 1990; Zabaras and Mukherjee 1987). The finite element method appeared preferable (Hwang et al. 1972; Shen 1988), since it permits easier treatment

Printed in Canada / Imprimé au Canada

of the nonlinear heat transfer and a straightforward extension to the coupled thermal–stress analyses, which is the future direction of the research.

In the following, the governing equations and the finite element formulation are illustrated first. Details are also provided on the time integration technique and on the procedure adopted to account for the latent heat during the water–ice transition. Then, the results of laboratory freezing tests carried out on large cylindrical sand samples are presented. These have been used to check the computer program and to evaluate the procedure used to determine the thermal properties of the sand.

Finally, the results of a parametric study illustrate the influence of pipe diameter, pipe separation, and coolant temperature on the advance of the 0°C isotherm.

A matrix notation is used herein to describe the numerical-solution approach. Boldface lowercase and uppercase letters denote vectors, and matrices, respectively. A dot above a term indicates a time derivative, and a superscript T means transpose.

2. Governing equations and boundary conditions

Before discussing the governing equations it is necessary to outline the assumptions used:

(*i*) the soil is saturated,

(*ii*) the thermal properties are not influenced by the stress and strain variation during freezing,

(*iii*) no seepage flow is permitted within the soil,

(*iv*) the volume increase due to freezing is neglected.

The first and second assumptions should not limit the application of the solution technique. The third assumption is necessary, since freezing would not be effective in the presence of significant water flow (Hashemi and Sliepcevich 1973). In fact, if an appreciable seepage velocity exists (say 1–2 m/day), artificial freezing would not be appropriate because of the continuous introduction of heat by the flowing water. To avoid this negative effect, the seepage within the soil should be prevented through adequate provisions before freezing. If no seepage flow exists, the "local" motion of water is restricted by the small size of pores and, hence, convection can be neglected.

It is worthwhile observing that eliminating the motion of pore water permits the use of the same governing equations for heat transfer within both the frozen and unfrozen soil.

The validity of the fourth hypothesis depends strongly on the characteristics of soil. In particular, it can be accepted for clean, coarse-grained soils. On the contrary, the behaviour of silt or clay during freezing is markedly influenced by the effects of moisture migration toward the freezing front due to frost heave. As a consequence, the use of the results of this work should be limited to clean sands or gravels.

With the above assumptions, the analysis of the freezing of saturated sand can be reduced to the so-called Stefan problem (see e.g., Carslaw and Jaeger 1959) or to the analysis of heat transfer by conduction within the soil undergoing phase changes (Nixon and McRoberts 1973).

In the following, the governing equations and the finite element formulation are discussed. The procedure for determining the thermal properties of sand, for a correct analysis of in situ freezing problems, will be discussed in a subsequent section.

The equation governing the two-dimensional flow of heat by conduction through an isotropic medium can be written in the following form (Carslaw and Jaeger 1959):

$$[1] \quad \frac{\partial}{\partial x}\left(k\frac{\partial T}{\partial x}\right)+\frac{\partial}{\partial y}\left(k\frac{\partial T}{\partial y}\right)+\bar{Q}=\rho c\frac{\partial T}{\partial t}$$

where x and y are the Cartesian axes; T and t denote temperature and time, respectively; k is the coefficient of thermal conductivity; ρ and c are the mass density and specific heat, respectively; and $\bar{Q}$ is the rate of internal heat generation per unit volume. Note that for the problem under examination the material parameters depend on temperature. The extensions of [1] to the axisymmetric and other conditions are given in Carslaw and Jaeger (1959).

If no phase change occurs, four main conditions can be imposed on portions of the boundary Γ of the flow domain Ω.

The temperature is known on Γ_1 (prescribed temperature, or "essential," condition) as

$$[2a] \quad T-\bar{T}(x,y,t)=0$$

and the heat-flow component normal to the boundary is prescribed on Γ_2 (heat-flow, or "natural," condition) as

$$[2b] \quad k\left(i_x\frac{\partial T}{\partial x}+i_y\frac{\partial T}{\partial y}\right)-\bar{q}_n(x,y,t)=0$$

where $\bar{q}_n$ and $\bar{T}$ represent, respectively, the imposed rate of heat flow per unit area and the prescribed temperature; and i_x and i_y are the direction cosines of the unit outward vector normal to the boundary.

The convection or radiation boundary conditions can be expressed by [2*b*] where $\bar{q}_n$ is replaced by the rates of heat flow per unit area associated with convection and radiation.

For phase transition a surface $F(x,y,t) = 0$ exists, having an a priori unknown shape, that separates the frozen and unfrozen zones. Similar to other moving-boundary problems (Crank 1984), this surface is characterized by two conditions: one on the free variable (i.e., the temperature) and one on its gradient. The first condition is that the temperatures of the unfrozen (T_u) and frozen (T_f) soil are equal to the melting–freezing temperature T_m:

$$[3a] \quad T_u(x,y,t) = T_f(x,y,t) = T_m$$

The second condition requires that the net rate of heat flow normal to the moving surface, the latent heat per unit volume, and the velocity v_n of the surface itself fulfill the relationship

$$[3b] \quad k_f\left(i_x\frac{\partial T_f}{\partial x}+i_y\frac{\partial T_f}{\partial y}\right)-k_u\left(i_x\frac{\partial T_u}{\partial x}+i_y\frac{\partial T_u}{\partial y}\right)=L\rho v_n$$

where k_f and k_u are the coefficients of thermal conductivity of frozen and unfrozen zones, respectively; L is the latent heat per unit mass; and ρ is the mass density.

3. Finite element formulation

3.1. Conduction problem without phase change

The finite element formulation of heat-conduction problems without phase changes (Zienkiewicz 1977; Lewis and Morgan 1983) will be considered first. The heat-flow domain Ω is subdivided into elements in which the temperature depends on the nodal values, for the eth element:

$$[4] \quad T_e(x,y,t) = b_e^T(x,y)\ T_e(t)$$

where T_e is the temperature within the element, and vec-

tors T_e and b_e collect, respectively, the nodal temperatures and the interpolation functions.

By writing [1] in the so-called weak form (Zienkiewicz 1977), and by considering the natural boundary conditions [2*b*], mathematical manipulations lead to the following matrix relationship for the entire finite element mesh:

$$[5] \quad M\,T + N\,\dot{T} = \bar{f}_\Omega + \bar{f}_\Gamma$$

Matrices and vectors in [5] are obtained by suitably overlapping the contributions of each element, denoted by the index e;

$$[6a] \quad M_e = \int_{\Omega_e} (\nabla b_e^T)^T K_e (\nabla b_e^T)\, d\Omega$$

$$[6b] \quad N_e = \int_{\Omega_e} b_e (\rho c)_e b_e^T\, d\Omega$$

$$[7a] \quad \bar{f}_{e\Omega} = \int_{\Omega_e} b_e \bar{Q}_e\, d\Omega$$

$$[7b] \quad \bar{f}_{e\Gamma} = \int_{\Gamma_{e2}} b_e \bar{q}_{en}\, dT$$

Here $\nabla^T = \{\partial/\partial x,\ \partial/\partial y\}$ is the linear differential operator, K_e is the 2×2 matrix of the thermal conductivity coefficients, and $i_e^T = \{i_x, i_y\}$ is the direction cosine vector (cf. [2*b*]). Vectors $\bar{f}_{e\Omega}$ and $\bar{f}_{e\Gamma}$ collect, respectively, the nodal heat flows due to internal heat generation per unit volume and those associated with the imposed rate of heat flow on Γ_{e2}. $\bar{q}_{en}$ is the imposed rate of heat flow $\bar{q}_n$ (c.f. (2*b*] for the eth finite element.

Before integrating with time the system of scalar equations [5], it is necessary to impose the essential boundary conditions expressed by [2*a*].

3.2. Time integration

The step by step time integration of [5] has been based on the assumption of linear variation of the time dependent variables within a time increment $\Delta t > 0$. This permits the rewriting of [5] in the following incremental form:

$$[8] \quad \left[\frac{\Delta t}{2}(M_{t+\Delta t}^{i-1} + M_t) + (N_{t+\Delta t}^{i-1} + N_t)\right] T_{t+\Delta t}^{i} = \Delta t(\bar{f}_{t+\Delta t}^{i-1} + \bar{f}_t) + \left[-\frac{\Delta t}{2}(M_{t+\Delta t}^{i-1} + M_t) + N_{t+\Delta t}^{i-1} + N_t)\right] T_t$$

where i denotes the iteration number and

$$\bar{f} = \bar{f}_\Omega + \bar{f}_\Gamma$$

Note that since matrices M and N are functions of temperature they are, in turn, functions of time.

At the beginning of the iterations for a time increment Δt all quantities at time t are known. Trial values of the nodal temperatures at time $t + \Delta t$ are extrapolated on the basis of those computed at the end of the preceding increments, and the relevant matrices and vectors are evaluated at time $t + \Delta t$. Then, improved values of the nodal temperatures at time $t + \Delta t$ are obtained through [8], and all matrices and vectors are recalculated. This iterative process terminates when the difference between the nodal temperatures at $t + \Delta t$ evaluated at two subsequent iterations decreases below a chosen lower limit.

3.3. Phase transition

The transition between solid and liquid phases is introduced in the solution of the Stefan problem by the boundary conditions [3] on the surface separating the frozen and unfrozen zones, which is also referred to as a moving boundary.

Some of the finite element approaches presented in the literature which can be referred to as variable mesh methods (Zabaras and Ruan 1989, 1990) explicitly take into account [3] in the calculations. They are conceptually similar to those applicable to unconfined seepage analyses (Gioda and Desideri 1988) and modify the geometry of the grid during the iterative solution process until a part of its boundary approximates with the required accuracy the shape of the moving surface at a chosen time.

Approaches of this type are usually rather accurate, but their use becomes exceedingly complex if several moving surfaces exist that tend to join with each other when freezing propagates. Since this situation is likely to occur when dealing with artificial freezing of ground, an alternative class of approaches, the so-called fixed-mesh techniques, has to be considered. They operate on a grid of constant geometry, hence the nodal coordinates remain unchanged during solution and allow the moving boundary to pass through the elements. Usually these procedures are less accurate than the preceding ones, but offer the nonnegligible advantage of handling several simultaneous moving surfaces without requiring particular programming provisions.

Various fixed-mesh procedures have been proposed in the literature for the solution of the Stefan problem (Voller et al. 1990). Some of them introduce the latent-heat effects through a variation of the heat capacity c within a given temperature range. They lead to satisfactory results if the phase change occurs in a relatively wide temperature interval, as in the case of alloys. However, if the change takes place at almost constant temperature, this procedure would involve a heat capacity versus temperature relationship similar to a Dirac function. Such a sharp variation could be overlooked by the time integration process, or could introduce some numerical instability, unless extremely small time increments are used, with a consequent large increase of computational time.

To limit this drawback, an alternative class of techniques was suggested (Comini et al. 1974; Morgan et al. 1978; Rolph and Bathe 1982) that adopts the enthalpy (i.e., the integral of the relationship between ρc and temperature) as a new variable. In fact, in the case of phase change at constant temperature, the enthalpy–temperature relationship approaches a step function, which should introduce less severe time integration problems than the previous Dirac-like function.

A technique different from the above was adopted in this study; it does not introduce a fictitious variation of the heat capacity nor does it require the use of enthalpy. The latent heat is viewed as a positive or negative source of heat, uniformly distributed on the volume, which becomes active when the freezing–melting temperature is reached, and that is accounted for in the finite-element analysis in integral form.

At the beginning of the calculations the nodal vector of total latent heat (q_L) is evaluated by the following equa-

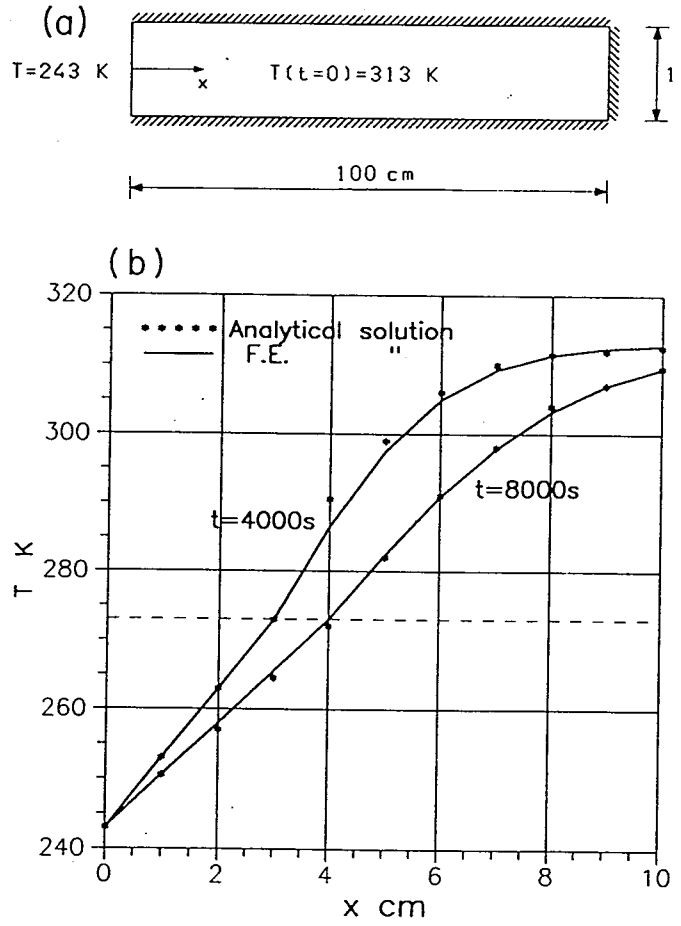

FIG. 1. (*a*) Scheme of the one-dimensional freezing problem (upper, lower, and right sides of the slab are impervious to heat; the temperature is prescribed on the left side. (*b*) Finite element (F.E.) and analytical temperature distributions for two time values.

tion, where the summation runs over the element of the mesh:

$$[9] \quad q_L = \Sigma_e \int_{\Omega_e} b_e L\rho \, d\Omega$$

Then, when the temperature of the nth node reaches the phase transition value, the node is "constrained" so that no further variation of its temperature may occur. The increments of nodal heat Δq_{nj} are then evaluated for each (jth) time step until the accumulated value reaches the previously evaluated nodal latent heat:

$$[10] \quad \Sigma_j \Delta q_{nj} = q_{nL}$$

When [10] is fulfilled the node is released and its temperature is again allowed to vary with time. If during a time step the accumulated nodal heat overcomes the corresponding latent heat, the node is released and a nodal heat increment is imposed equal to the difference between the previously accumulated heat and the total latent heat.

This technique is apparently more "robust" than those based on the fictitious variation of the heat capacity or on the enthalpy approach. In fact, it is not affected by possible numerical instability caused by Dirac and step functions and, hence, relatively large steps can be adopted for time integration. On the other hand, it involves perhaps more computer time because of the matrix manipulations required for constraining the nodes that reach the freezing temperature.

Some test problems were solved to check the accuracy of this technique. They showed that the numerical analysis can provide reasonably precise results, from an engineering viewpoint, with an acceptable computational effort. As an example, the numerical solution of a one-dimensional problem is shown in Fig.1 and compared with the corresponding analytical solution reported by Comini et al. (1990).

4. Experimental investigation

To apply the described solution technique to actual engineering problems, it is necessary to evaluate the equivalent thermal parameters of the sandy soil. This is not an easy task. In fact, various procedures have been suggested in the literature that do not lead to unique values of these parameters. In addition, once one of them has been chosen, it is difficult to assess a priori the accuracy of the consequent numerical results.

To overcome this problem some laboratory freezing tests were performed to check the computer program and to choose a suitable procedure for determining the equivalent thermal parameters.

4.1. Equipment characteristics and deposition of sand

The experimental setup consists of a thermally insulated cylinder, having internal diameter and height of 1 m, filled with saturated sand of uniform density. A steel pipe, installed at the centre of the container, is used for the circulation of liquid nitrogen. The vertical and horizontal sections of the equipment are shown in Fig 2.

The cylindrical geometry of the container and its insulation, consisting of polyurethane foam, lead to axisymmetric and planar heat-flow conditions during the tests. This permits easier interpretation of the experimental results by the finite-element analysis.

The soil used in the tests was obtained by mixing predefined quantities of four sands having almost constant grain size. This eliminates the presence of silt (and the related problems caused by the migration of water towards the frost front) and leads to the well-graded grain-size distribution shown in Fig. 3.

Before the deposition of sand about 10 cm of water was placed in the container. Then deposition was initiated by spreading the sand from a sieve kept at a constant level above the water surface. Additional water was introduced during deposition to maintain the water level about 10 cm above the deposed sand. This technique led to a saturated soil having a fairly uniform density throughout the container.

The same technique was adopted for preparing small samples for density measurements. The water content ranged between 0.279 and 0.30, the dry unit weight between 14.3 and 14.6 kN/m^3, and the porosity between 0.417 and 0.436.

A small gap of about 2 cm was left between the sand and the top of the container to avoid possible damage caused by the volume increase of water during freezing. Drainage was allowed using three small-diameter pipes inserted in the container wall at the level of the 2 cm gap. Because of an iron oxide impurity, the freezing temperature of water, determined using a cryoscope, was −0.5°C.

During the deposition of sand nine thermal transducers were placed at mid-height of the container, to reduce the disturbance due to the upper and lower bases. They were located along three radii, at an angle of 120° from each other and at distances of 150, 270, and 390 mm from the centre.

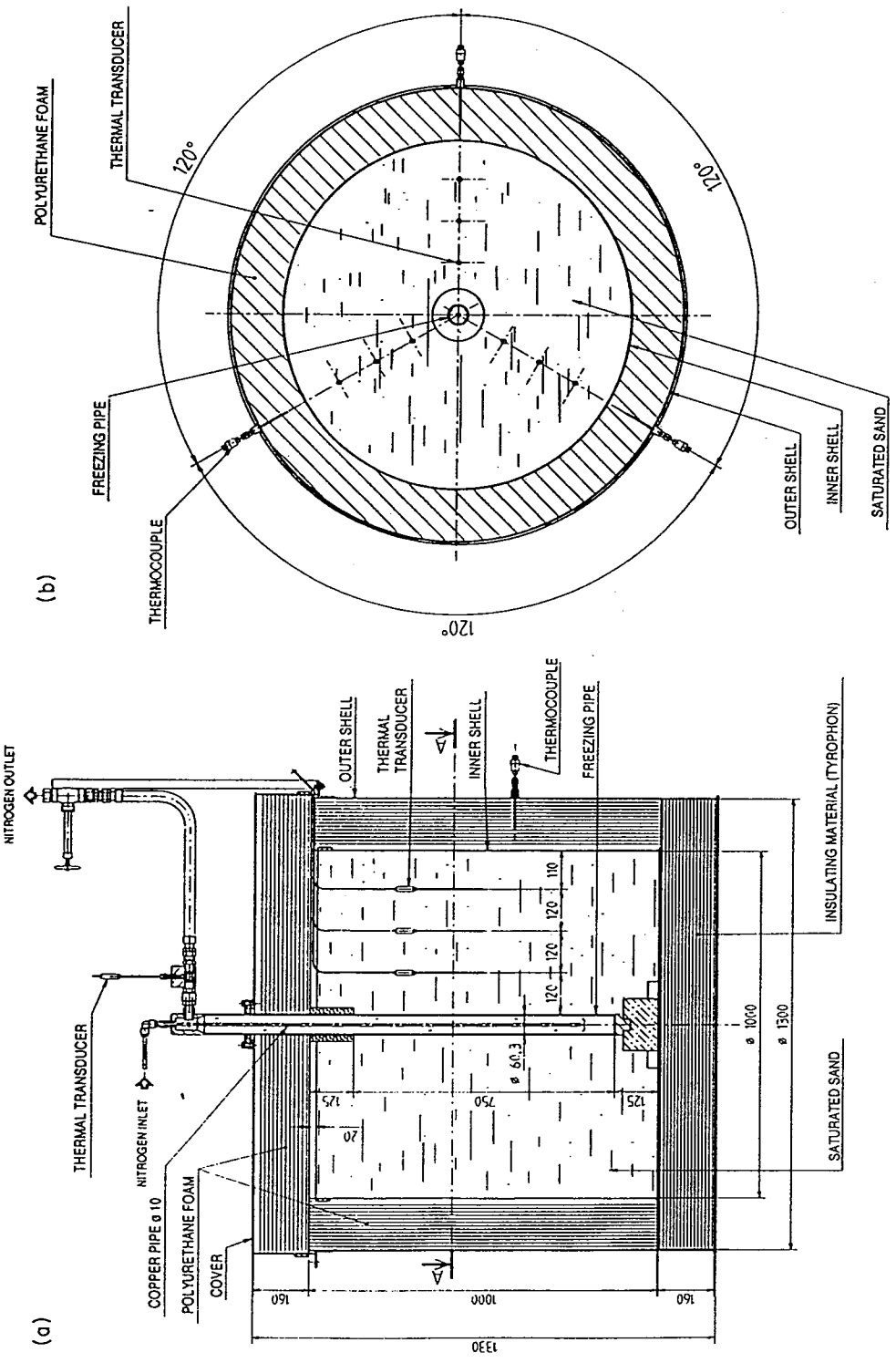

FIG. 2. (*a*) Vertical section of the equipment used for the laboratory freezing tests. All dimensions are in millimetres. (*b*) Horizontal section through A–A in *a*.

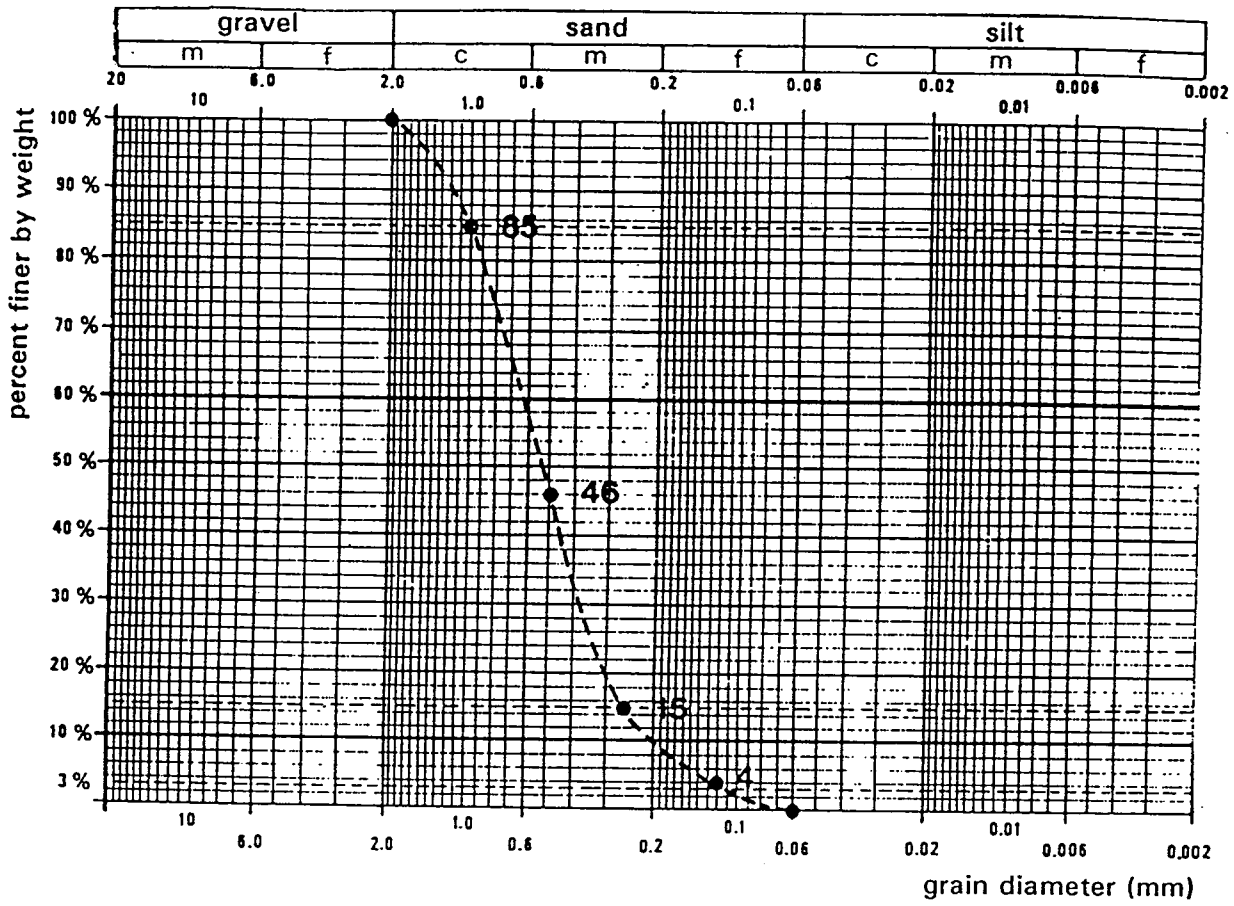

FIG. 3. Grain-size curve of the sand used in the freezing tests.

Three additional transducers were used to measure the temperature of the room, of the nitrogen at its outlet from the steel pipe, and the outer part of the insulation. They operate from about −200 up to +500°C, with an accuracy higher than 0.5°C. Two thermocouples were also introduced within the polyurethane foam to check the effectiveness of the thermal insulation.

The 12 transducers were connected to a personal computer for data acquisition and storage. An overall view of the assembled equipment and of the data-acquisition unit is shown in Fig. 4.

4.2. Results of the freezing tests

Three tests were performed using pipes with external diameters of 33.7, 60.3, and 88.9 mm. These are commercially available pipes that have been used in actual freezing projects. In particular, the 60.3 mm diameter pipes are commonly used in practice.

The initial temperature of the soil ranged between 18 and 19°C. To facilitate the subsequent interpretation of the experimental data, the nitrogen flux was regulated in such a way that a constant temperature of −183°C was monitored at the pipe outlet.

For the sake of briefness only the results of the first test will be presented. The results of the other two tests will be shown subsequently together with those obtained by the numerical analyses.

The variation with time of the readings of the thermal transducers is shown in Fig. 5. Curves *a*, *b* and *c*, representing the temperatures within the sand, were obtained by averaging the readings of the transducers at the same distance from the axis. Only two transducers did not operate properly during two tests and were neglected. The maximum temperature difference measured at different radii at the same distance from the pipe was less than 1.5°C. This indicates that the heat flow within the container was close to the expected axisymmetric conditions.

The remaining curves in Fig. 5 represent the room temperature (*d*) and the temperature of the outer part of the insulating material (*e*). The polyurethane foam provided adequate thermal insulation, since its temperature is influenced by the room temperature, but it is barely affected by the temperature inside the container.

The coolant flux was stopped when the transducers farthest from the pipe reached 0°C. This avoided damage to the container due to the volume increase. In fact, some litres of water had already escaped the cylinder through the drainage pipes before reaching this condition.

The recorded data show that after some hours the temperature of all transducers reached the same value (about −1°C), which remained practically constant for several days until the equipment was dismantled; this indicated that the polyurethane foam provided adequate thermal insulation.

5. Analysis of the experimental results

It was pointed out that heat flow inside the container is in the radial direction only and that, consequently, the numerical analyses can be performed in plane (normal to the cylinder axis) and axisymmetric conditions. On this basis, a one-dimensional finite element mesh was adopted consisting of a "line" of 50 four-node quadrilateral elements, each 1 cm in length so that the total length of the mesh coincides with

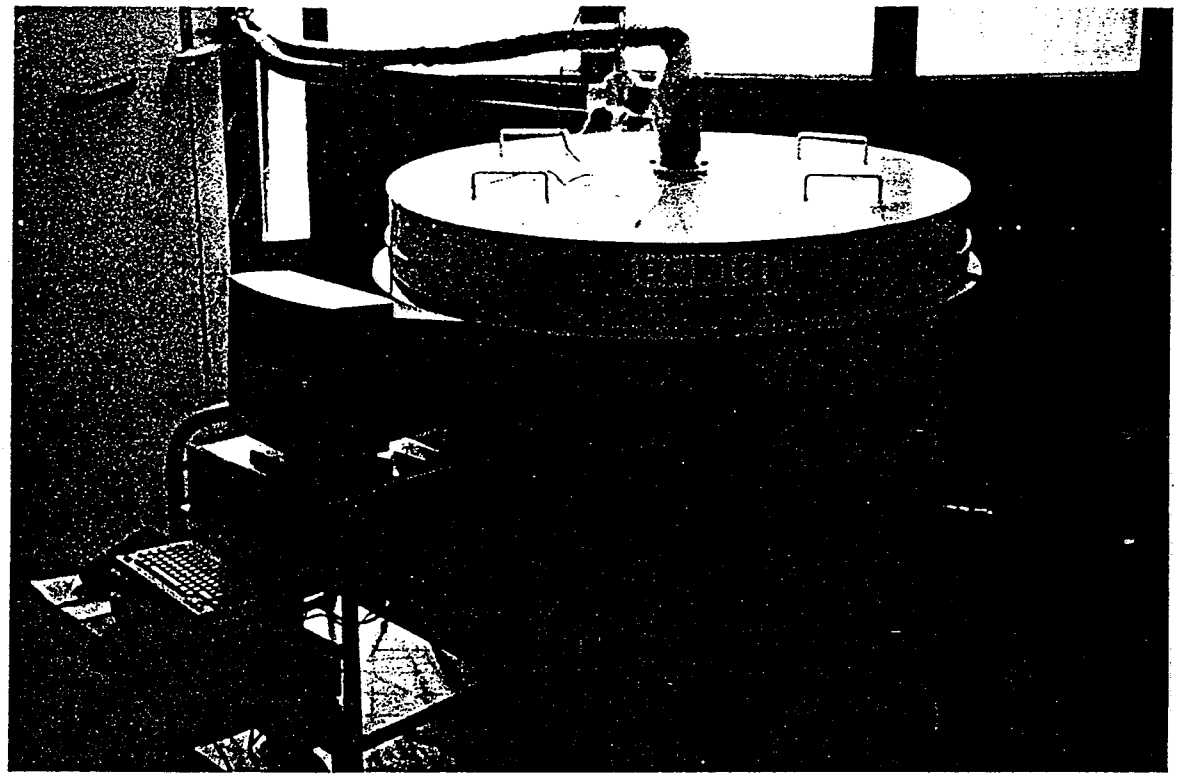

FIG. 4. Overall view of the equipment and the data-acquisition unit used for the freezing tests.

the inner radius of the container. The element height is constant throughout the mesh and does not affect the numerical results. All sides of the mesh were considered impervious to heat except for that adjacent to the freezing pipe, at which a temperature of −183°C was imposed.

Having defined the scheme for the finite element analyses, there is a major problem in determining the values of the thermal parameters characterizing the homogeneous medium equivalent to the saturated sand, including thermal conductivity k, thermal capacity c, and latent heat per unit mass L. For convenience, these parameters are expressed as follows both SI units and in terms of calories, grams, seconds and degrees Celsius:

k_{water} = 0.56 W/(m·K) = 0.001 338 cal/(s·cm·°C),
k_{ice} = 2.3 W/(m·K) = 0.005 495 cal/(s·cm·°C),
c_{water} = 4186 J/(kg·K) = 1.0 cal/(g·°C),
c_{ice} = 2060 J/(kg·K) = 0.492 1 cal/(g·°C),
L = 3.33 10^5 J/kg = 79,55 cal/g.

Although the thermal parameters of water are known with a high degree of accuracy, those of dry sand are more uncertain, owing to the marked influence of the mineralogic characteristics. From the literature, the following ranges of variation for thermal capacity and conductivity can be assumed,

k_{sand} = 0.27 ÷ 3.0 W/(m·K) = 0.00063 ÷ 0.007 cal/(s·cm·°C)
c_{sand} = 600 ÷ 800 J/(kg·K) = 0.15 ÷ 0.19 cal/(g·°C)

A suggested average value for c is

c_{sand} (avg.) = 710 J/(kg·K) = 0.17 cal/(g·°C).

The thermal properties of the saturated soil can be evaluated according to Kersten (1949). In particular, the thermal capacity depends on the thermal properties of the minerals constituting the sand and of the water (or ice), and on the water content w. Hence, the equivalent thermal capacities below and above freezing are

[11a] $c_{frozen} = c_{sand} + wc_{ice}$

[11b] $c_{unfrozen} = c_{sand} + wc_{water}$

In the above relationships, c_{sand} is the thermal capacity of the dry sand, which was assumed equal to the above-mentioned average value.

The equivalent latent heat (per unit mass) L_{eq} is defined as the product of the latent heat of the water L by the water content w:

[12] $L_{eq} = Lw$

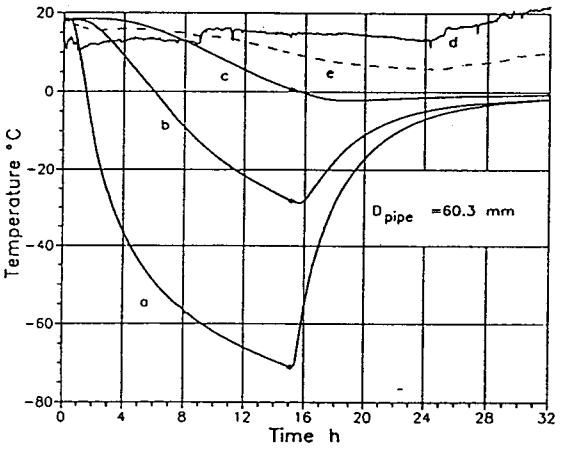

FIG. 5. Temperature vs. time data from the test with pipe diameter D_{pipe} = 60.3 mm. Temperatures of the transducers located at (*a*) 150, (*b*), 270, and (*c*) 390 mm from the cylinder axis. *d*, room temperature; *e*, temperature of outer thermal insulation. *, end of liquid nitrogen flow.

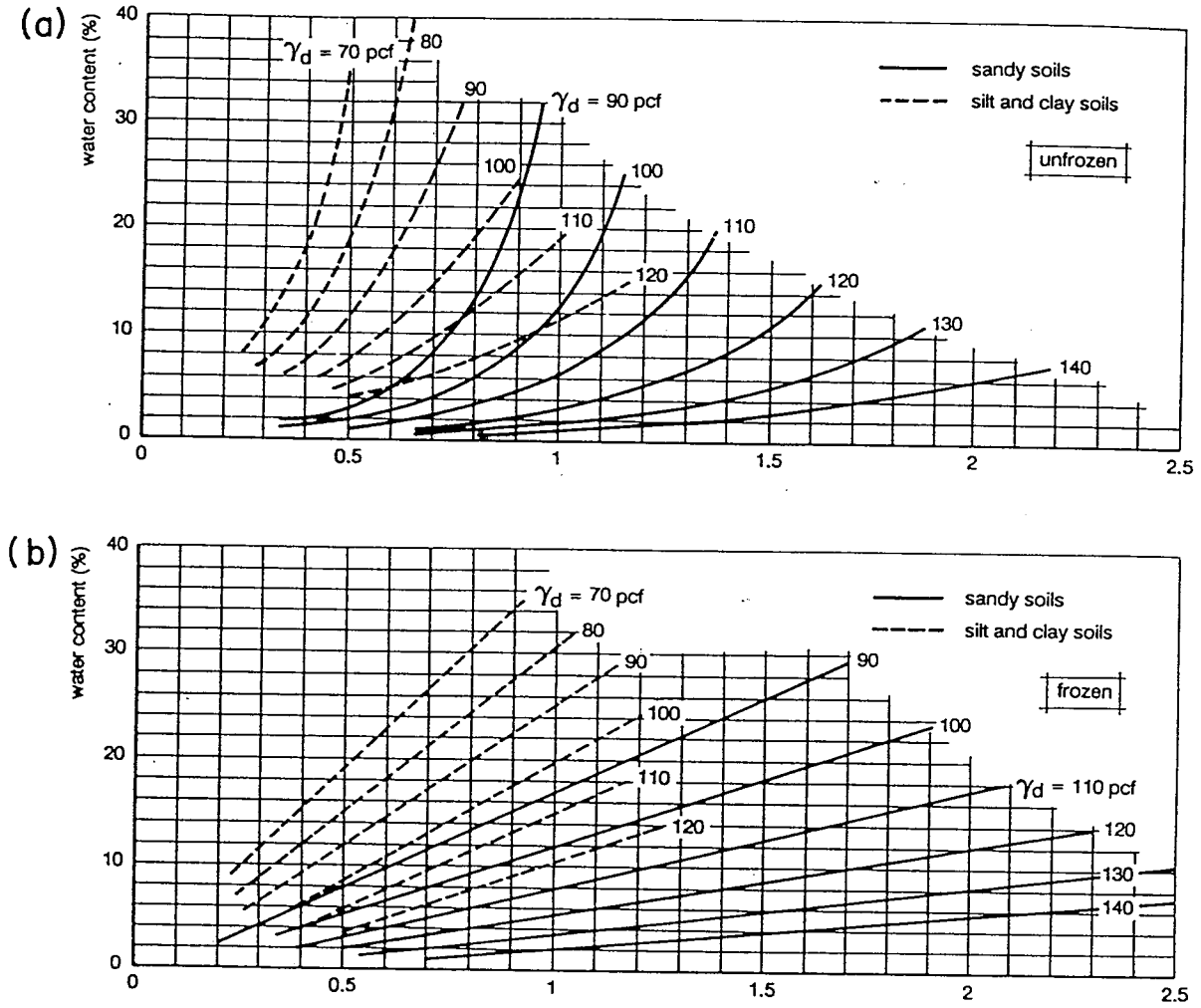

FIG. 6. Relationship between thermal conductivity and water content for (*a*) unfrozen (K_u) and (*b*) frozen (K_f) soils (after Kersten 1949), measured as BTU (min. f °F)$^{-1}$, where 1 BTU (min ft °F)$^{-1}$ = 1.73 W (m·K)$^{-1}$. pcf, pounds per cubic foot (1 pcf = 0.016 t/m); γ_d, dry unit weight of soil.

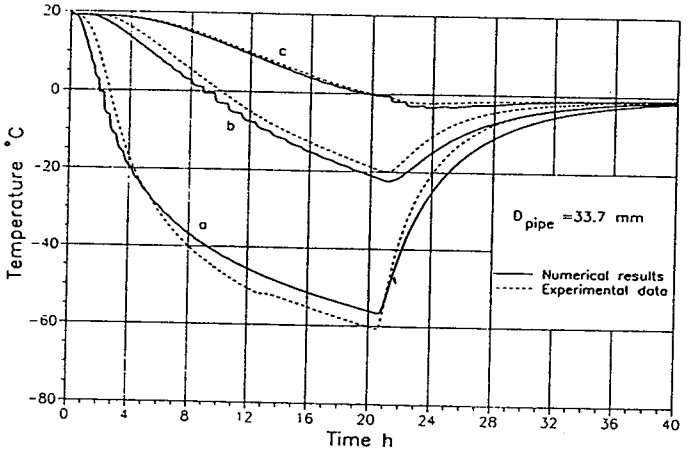

FIG. 7. Comparison between experimental and numerical temperature vs. time data for the test with pipe diameter D_{pipe} = 33.7 mm. Temperatures of the transducers located at (*a*) 150, (*b*) 270, and (*c*) 390 mm from the cylinder axis.

The procedure for evaluating the equivalent thermal conductivity is less straightforward than the procedures used for evaluating c and L. A first attempt was based on the diagrams proposed by Kersten (1949) (cf. Fig. 6), which provide the conductivity as a function of water content and type of soil.

Unfortunately, when adopted in the numerical analyses, this procedure led to results only qualitatively similar to those of the experimental data. It was decided, then, to modify the method for evaluating the conductivity and to adopt the suggestion by Johansen and Frivik (1980). In this case the equivalent parameter k depends on the conductivity of the water (or ice), on that of quartz k_q, and on that of the remaining fraction of sand k_r through the following expressions which hold for temperatures below and above freezing, respectively:

$$[13a] \quad k_{frozen} = k_{ice}^{n} \left(k_q^q \, k_r^{(1-q)}\right)^{(1-n)}$$

$$[13b] \quad k_{unfrozen} = k_{water}^{n} \left(k_q^q \, k_r^{(1-q)}\right)^{(1-n)}$$

In using [13], where q is the content of quartz and n the porosity of the sand, the following values of the relevant parameters were adopted: k_q = 7.7 W/(m·K), k_r = 2.5 W/(m·K), and q = 50%. It was also taken into account that the thermal conductivity of ice undergoes a non-negligible variation when the temperature decreases well below the freezing point. To account for this effect, the following linear interpolation of the experimetnal data was adopted relating k_{ice} (W/(m·K)) to temperature (°C) (Frivik and Thorbergsen 1980):

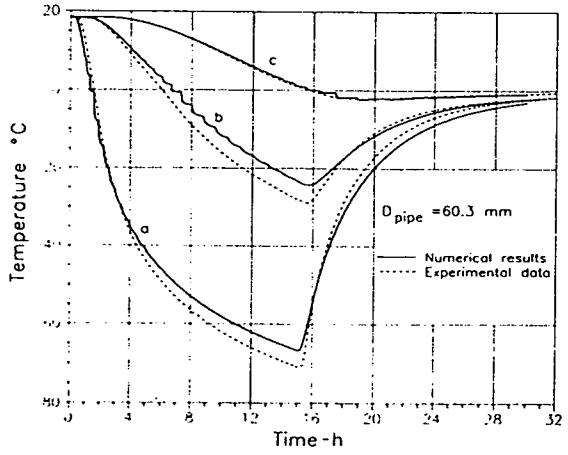

FIG. 8. Numerical and experimental results for the tests with pipe diameter D_{pipe} = 60.3 mm (other data as in Fig. 7).

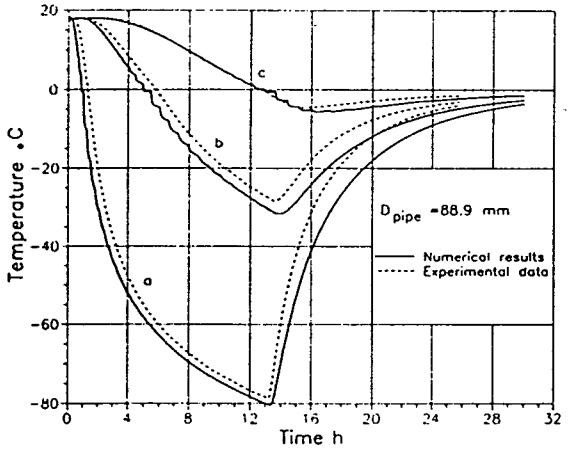

FIG. 9. Numerical and experimental results for the tests with pipe diameter D_{pipe} = 88.9 mm (other data as in Fig. 7).

[14] $k_{ice} = 2.3 - 0.015\ T$

Equations [11]–[14] have been introduced in the finite element simulation of the freezing tests, obtaining results that are shown in Figs. 7–9 together with the corresponding experimental data. The only difference between the material parameters used in the three analyses depends on the slightly different relative density of sand.

The comparison between experimental and numerical results indicates that the finite element calculation is able to provide an acceptable estimation, from an engineering standpoint, of the heat flow within the sand and that also the progress of the 0°C isotherm is evaluated with reasonable accuracy.

It is perhaps worthwhile to observe that the stepwise pattern of the numerical diagrams in the vicinity of the phase-change temperature depends on the particular procedure adopted for taking into account the latent-heat effects.

6. Effect of diameter and distance of the freezing pipes

Among the geometrical parameters that influence in situ freezing are the diameter of the pipes and the distance among them. To investigate their effect, a parametric study was performed based on the developed finite element program.

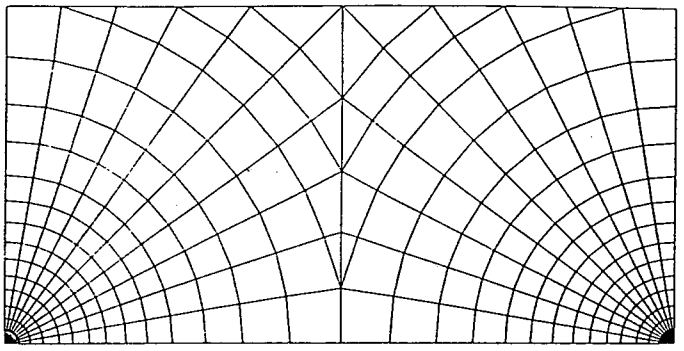

FIG. 10. Mesh of isoparametric quadrilateral four-node elements for the two-dimensional analysis of freezing induced by a square pattern of pipes.

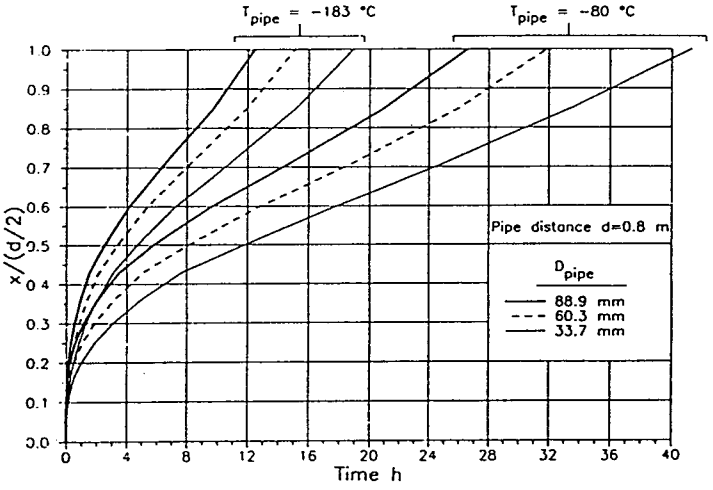

FIG. 11. Results of the problem in Fig. 10. Variation with time of the distance x between pipe axis and corresponding frozen front for various coolant temperatures T and pipe diameters D. Initial soil temperature T_0 = 20°C.

The finite element mesh adopted in the calculations is depicted in Fig. 10, which represents a horizontal section of a portion of a grid of regularly spaced pipes. The temperature of the coolant is imposed at the external surface of the pipes, while the remaining boundaries of the mesh, the symmetry of the problem being taken into account, are considered impervious to heat.

In these calculations the material parameters coincide with those used in the analysis of the laboratory test with the 60.3 mm diameter pipe. The initial temperature of the soil is 20°C.

The results of the parametric study are summarized in Figs. 11 and 12 through diagrams relating the progress of the frozen front, in terms of the nondimensional quantity $x/(d/2)$, with time. Here d represents the distance between the axis of two adjacent pipes, and x is the distance between the pipe axis and the corresponding 0°C isotherm. Consequently, the frozen fronts of two adjacent pipes join with each other when $x/(d/2) = 1$. Note that in situ freezing is commonly carried out using 60.3 mm diameter pipes and that the distance between them is about 80 cm.

Figure 11 shows two sets of curves corresponding, respectively, to coolant temperatures of −183 and −80°C. With reference to actual field conditions these temperatures refer to pipes close to, and far away from, the inlet of liquid

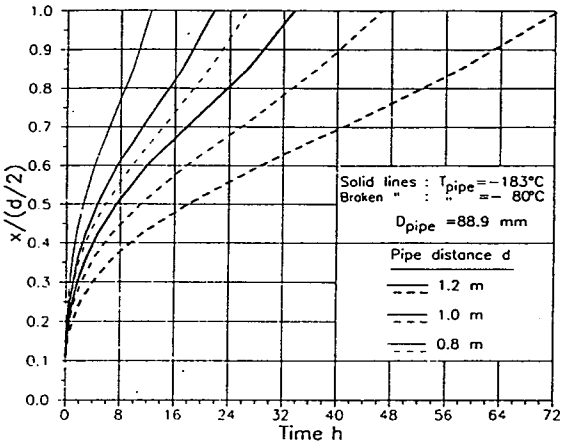

FIG. 12. Results of the problem in Fig. 10. Variation with time of the distance x between pipe axis and corresponding frozen front for various coolant temperatures T and pipe distances d. Initial soil temperature T_0 = 20°C.

nitrogen. The curves within each set correspond to pipes having external diameters of 88.9, 60.3, and 33.7 mm.

The diagrams in Fig. 12 refer only to 88.9 mm diameter pipe. They show the progress of the 0°C isotherm with time for different relative distances d of the pipes (i.e., 1.2, 1.0, and 0.8 m). Again the temperature of the coolant is equal to −183 and to −80°C.

The results of this parametric study clearly show the influence of pipe distance and diameter on the rate of freezing. For instance, when d = 80 cm the time required for two frozen fronts to join decreases by about 19% if the diameter of the pipes increases from 60.3 to 88.9 mm. On the contrary, a reduction of the diameter from 60.3 to 33.7 mm leads, for the same value of d, to a time increment of about 24–28%. When large-diameter pipes are used (88.9 mm), a time increment of about 75% is produced if the distance between them increases from 0.8 to 1.0 m and goes up to more than 180% if the distance increases to 1.2 m.

7. Conclusions

A study of the nonlinear conduction of heat within saturated sand has been presented, with reference to the analysis of the artificial freezing of soils. The purpose of this study was to develop a finite element technique that can be adopted in parametric investigations for "optimizing" some of the parameters that characterize the freezing system.

A series of laboratory freezing tests on large samples was carried out, the results of which permitted a check on the accuracy of the developed computer program and provided a convenient procedure for determining the thermal constants of the soil. A parametric study has been also presented that illustrates the effects of the diameter of the freezing pipes, the distance between the pipes, and the temperature of the coolant on the progress of the frozen front.

On the basis of these results it is concluded that the developed numerical procedure is able to solve heat-transfer problems related to ground freezing with an acceptable accuracy from an engineering viewpoint. As expected, the parametric study indicates that the diameter of the pipes and the distance between them have a marked influence on the time required by the freezing process. Since a reduction of time can appreciably influence the cost and, hence, the design of the freezing system, further study on the optimization of the mentioned quantities through more detailed parametric investigations is needed.

Acknowledgements

The authors wish to thank Dr. Astorri (SIO s.r.l.) and Mr. Bassi (Rodio S.p.A.) for their helpful co-operation, and Dr. Granata and Mr. Anelli (Rodio S.p.A.) for their invaluable contribution to the design of the experimental equipment.

Andersland, O.B., Gallavresi, F., Goto S., Saareleinen, S., and Slunga. E. 1989. General report of the specialty session on ground freezing. *In* Proceedings of the 12th International Conference on Soil Mechanics and Foundation Engineering, Rio de Janeiro, 13–18 Aug. 1989. *Edited by* Comité des Publications du XII CIMSTF. Balkema, Rotterdam, vol. 4, pp. 2657–2672.

Carslaw, H.S., and Jaeger, J.C. 1959. Conduction of heat in solids. 2nd ed. Oxford University Press, Oxford, U.K.

Comini, G., Del Giudice, S., Lewis, R.W., and Zienkiewicz, O.C. 1974. Finite element solution of non-linear heat conduction problems with special reference to phase change. International Journal of Numerical Methods in Engineering, **8**: 613–624.

Comini, G., Del Giudice, S., and Saro, O. 1990. A conservative algorithm for multidimensional conduction phase change. International Journal of Numerical Methods in Engineering, **30**: 697–709.

Crank, J. 1984. Free and moving boundary problems. Oxford University Press, Oxford, U.K.

Del Giudice, S., Comini, G., and Lewis, R.W. 1978. Finite element simulation of freezing process in soils. International Journal of Numerical and Analytical Methods in Geomechanics, **2**: 223–235.

Frivik, P.E., and Thorbergsen, E. 1980. Thermal design of artificial soil freezing systems. *In* Proceedings of the 2nd International Symposium on Ground Freezing, Trondheim, Norway, 24–26 June. *Edited by* P.E. Frivik, N. Jambu, R. Saetersolal, and L.I. Finborud. Elsevier, Amsterdam, vol. 1, pp. 556–567.

Gioda, G., and Desideri, A. 1988. Some numerical techniques for free surface seepage analysis. *In* Proceedings of the 6th International Conference on Numerical Methods in Geomechanics, Innsbruck, Austria, 11–15 April. *Edited by* G. Swoboda. Balkema, Rotterdam, vol. 1, pp. 71–84.

Hashemi, H.T., and Sliepcevich, C.M. 1973. Effect of seepage stream on artificial soil freezing. ASCE Journal of the Soil Mechanics and Foundation Division, **99**(SM3): 267–289.

Hwang, C.T., Murray, D.W., and Brooker, E.W. 1972. A thermal analysis for structures on permafrost. Canadian Geotechnical Journal, **9**: 33–46.

Johansen, O., and Frivik, P.E. 1980. Thermal properties of soils and rock materials. *In* Proceedings of the 2nd International Symposium on Ground Freezing, Trondheim, Norway, 24–26 June. *Edited by* P.E. Frivik, N. Jambu, R. Saetersolal, and L.I. Finborud. Elsevier, Amsterdam, vol. 1, pp. 427–453.

Kersten, M.S. 1949. Laboratory research for the determination of the thermal properties of soils. Final report, Engineering Experiment, Station, University of Minnesota, Minneapolis.

Lewis, R.W., and Morgan, K. (*editors*). 1983. Numerical methods in thermal problems. Pineridge Press, Swansea, U.K.

Morgan, K., Lewis, R.W., and Zienkiewicz, O.C. 1978. An improved algorithm for heat conduction problems with phase change. International Journal of Numerical Methods in Engineering, **12**: 1191–1195.

Nixon, J.F., and McRoberts, E.C. 1973. A study of some factors affecting the thawing of frozen soil. Canadian Geotechnical Journal, **10**: 439–452.

Rolph, W.D., and Bathe, K.J. 1982. An efficient algorithm for analysis of nonlinear heat transfer with phase change. International Journal of Numerical Methods in Engineering, **18**: 119–134.

Sanger F.J. 1968. Ground freezing in construction. ASCE Journal of the Soil Mechanics and Foundation Division, 94(SM1): 131–158.

Shen, M. 1988. Numerical analysis of temperature field in a thawing embankment in permafrost. Canadian Geotechnical Journal, 25: 163–166.

Voller ,V.R., Swaminathan, C.R., and Thomas B.G. 1990. Fixed grid techniques for phase change problems: a review. International Journal of Numerical Methods in Engineering, 30: 875–898.

Zabaras, N., and Mukherjee, S. 1987. An analysis of solidification problems by the boundary element method. International Journal of Numerical Methods in Engineering, 24: 1879–1900.

Zabaras, N., and Ruan, Y. 1989. A deforming finite element method analysis of inverse Stefan problem. International Journal of Numerical Methods in Engineering, 28: 295–313.

Zabaras, N., and Ruan Y. 1990. Moving and deforming finite element simulation of Stefan problem. Communications in Applied Numerical Methods, 6: 495–506.

Zienkiewicz, O.C. 1977. The finite element method. 3rd ed. McGraw-Hill, London, U.K.